

LANDSLIDES IN INTERIOR LAYERED DEPOSITS, VALLES MARINERIS, MARS: EFFECTS OF WATER AND GROUND SHAKING ON SLOPE STABILITY. D. P. Neuffer¹ and R. A. Schultz, Geomechanics-Rock Fracture Group, Department of Geological Sciences and Engineering/172, Mackay School of Earth Sciences and Engineering, University of Nevada, Reno, NV 89557-0138, ¹neufferd@mines.unr.edu.

Summary: We identified 12 landslides or landslide complexes derived from interior layered deposits (ILDs) in the Hebes, East Candor, and Melas Chasmata of Valles Marineris, Mars. Using slope stability analysis, we modeled five landslides to determine the possible failure mechanisms (Fig. 1). Three of the landslides could have failed readily under dry, static (e.g., current) conditions. One landslide in East Candor Chasma most likely required seismic ground acceleration to fail. A slope failure in Melas Chasma probably resulted from the release of subsurface fluids onto the ILD slope directly above the landslide.

Introduction: The ILDs of Valles Marineris are generally accepted to consist of “soft” volcanic or sedimentary rocks [1-6]. Most hypotheses for the origin of the ILDs involve deposition in water, such as lacustrine sedimentation [1-4] or subice/subaqueous volcanism [1,3,5,6]. Hence, determining the origin of the ILDs is vital to understanding the spatial and temporal distribution of water in the Valles Marineris region.

Several possible mass-wasting deposits emanating from ILDs have been identified in the Candor and Melas Chasmata [7-11]. Our search revealed over 60 possible landslides in central Valles Marineris, from which we positively identified 12 slides. Slope failures may be triggered by many processes, but are often initiated by changes in pore fluid pressure. Thus, the hydrologic conditions acting on a slope at the time of failure can be estimated from back-analysis of landslides. Slope stability analyses of intact ILD slopes have been performed previously [12], but landslides in ILDs have not been mechanically analyzed. We assessed the stability of five failed ILD slopes to evaluate different failure mechanisms, including the presence of water. Other confirmed landslides could not be modeled due to multiple failure episodes or poor preservation.

Approach: Limit equilibrium analysis is commonly used in geotechnical engineering to assess the stability of slopes. If the geometry, material strengths, pore fluid pressures, and ground acceleration are known for a given slope, the safety factor (SF) for that slope may be determined. The SF is the ratio of forces resisting movement to the forces driving movement of the portion of a slope that is most prone to fail. Hence, slopes with a SF less than one are unstable and slopes with a SF greater than one are stable. Limit equilib-

rium back-analysis is used to determine the conditions at the time of failure, where $SF = 1.0$. Slide is a slope stability program that uses two-dimensional limit equilibrium analysis to determine the SF for landslides with circular failure surfaces, such as those observed in the ILDs.

Because material strengths are unknown for the ILDs, we used lower bound terrestrial rock mass strengths for sandstone, shale, welded tuff, nonwelded tuff, and basalt from rock engineering literature [13-16] and hyaloclastite breccia strengths from previous work [17]. The Hoek-Brown strength criterion [18] accounts for the fractured nature of rock masses by incorporating Geologic Strength Index (GSI), in addition to the intact Unconfined Compressive Strength and intact material parameter, m_i , into strength envelope calculations. GSI ranges from 1 (highly weathered soil) to 100 (intact rock). The lower bound GSI values are 30, 10, 12, 55, 60, and 43 for sandstone, shale, welded tuff, nonwelded tuff, hyaloclastite breccia, and basalt rock masses, respectively. The lower bound UCS values (in MPa) are 25, 11, 12, 6, 24, and 142 for sandstone, shale, welded tuff, nonwelded tuff, hyaloclastite breccia, and basalt, respectively.

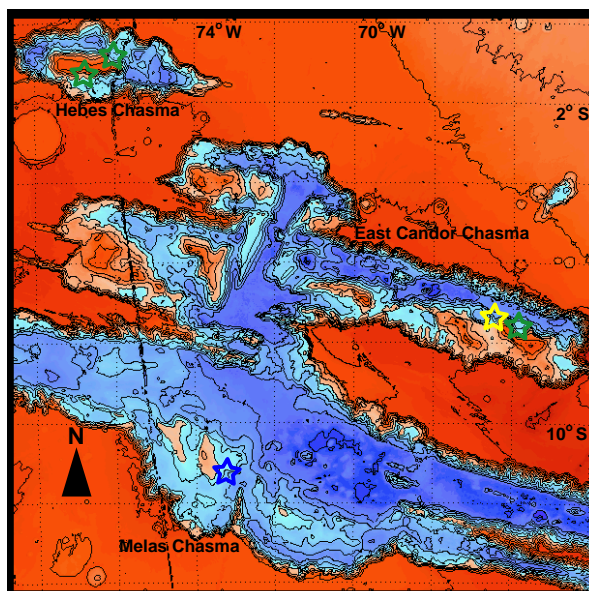


Figure 1. Location map of modeled ILD landslides. Blue and yellow stars denote landslides probably triggered by water and seismic loading, respectively. Green stars show landslides that could have failed under dry, static conditions. Contours are 1 km.

Utilizing Slide, we back-analyzed estimated pre-failure ILD slopes derived from a custom MOLA DEM [19]. Where slopes were predominantly stable under dry conditions, MOLA DEM, MOC, and THEMIS images were examined for evidence of triggering agents such as faults or fluids. We used slope stability modeling to assess the role of possible triggering agents in causing slope instability.

Results and Implications: Slope stability back-analyses show that the two Hebes Chasma landslides and one landslide in East Candor Chasma (Fig. 1) could have failed under dry, static conditions for the sandstone, shale, and both tuff rock mass strengths. If the ILD rock masses comprising the failed slopes were stronger than the representative strengths, or consisted of hyaloclastite breccia or basalt similar in strength to the terrestrial examples, water or ground shaking would have been involved in landslide initiation.

Analysis of one East Candor Chasma landslide (Fig. 1) suggests that seismic loading by a nearby fault under dry (e.g., present-day conditions) was the most likely triggering mechanism, as there is no geomorphic evidence for the presence of fluids. Also, low thermal inertia material blankets the chasma floor ahead of the slide toe, possibly indicating an airblast cloud similar to terrestrial dry rock avalanches. Slope stability back-analyses and preliminary peak ground accelerations estimated from empirical relationships [20,21] show that the trough-bounding normal fault ~20 km to the north of the landslide (Fig. 1) could produce the ground shaking necessary for failure of a dry slope for the sandstone, shale, welded and nonwelded tuff, and hyaloclastite breccia rock mass strengths.

For the landslide in Melas Chasma, geomorphic evidence and slope stability modeling indicate that failure was probably caused by a release of subsurface fluids from the slope above the landslide. A surface channel originating at an elevation of ~240 m is truncated by the landslide scarp at ~400 m, suggesting that released fluids eroded a channel in the ILDs and saturated the slope, causing instability. Back-analyses show that if the slope was saturated with water, failure would occur for the shale, welded tuff, and nonwelded tuff rock mass strengths (Fig. 2). Horizontal ground accelerations of 9, 76, and 137 cm/s² would be required for failure of a saturated slope for the sandstone, hyaloclastite breccia, and basalt rock mass strengths, respectively. The fluid release point implies a minimum equipotential surface elevation of ~240 m for an aquifer in this Melas ILD (Fig. 1). The channel and landslide cut ILDs; hence, the aquifer existed no earlier than the Late Hesperian to Early Amazonian [22].

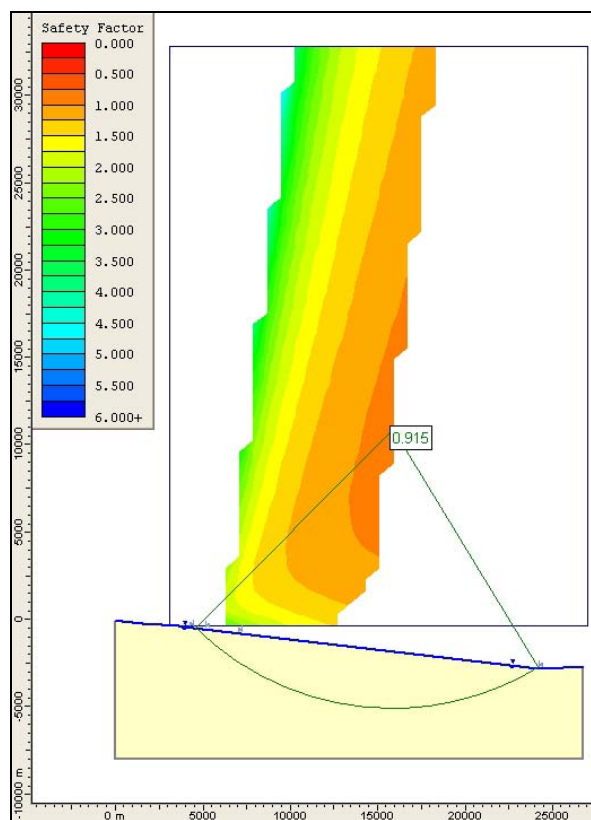


Figure 2. Slide model of the estimated pre-failure slope for the Melas Chasma landslide. The figure shows failure for a water-saturated slope consisting of nonwelded tuff.

- References:** [1] Nedell S. S. et al. (1987) *Icarus*, 70, 409-441. [2] Komatsu G. et al. (1993) *JGR*, 98, 11105-11121. [3] Lucchitta B. K. et al. (1994) *JGR*, 99, 3783-3798. [4] Malin M. C. and Edgett K. S. (2000) *Science*, 290, 1927-1937. [5] Chapman M. G. and Tanaka K. L. (2001) *JGR*, 106, 10087-10100. [6] Komatsu G. et al. (2004) *PSS*, 52, 167-187. [7] Lucchitta B. K. (1990) *Icarus*, 86, 476-509. [8] Lucchitta B. K. (1996) *LPS XXVII*, 779-780. [9] Lucchitta B. K. and Rosanova C. E. (1997) *LPS XXVIII*, Abstract #1512. [10] Lucchitta B. K. (2001) *LPS XXXII*, Abstract #2059. [11] Skilling I. P. et al. (2002) *LPS XXXIII*, Abstract #1361. [12] Schultz R. A. (2002) *GRL*, 29(19), 1932. [13] Hoek E. et al. (1998) *Bull Eng Geol Env*, 57, 151-160. [14] Dalgic S. (2000) *Eng Geol*, 58, 137-148. [15] Ozsan A. and Basarir H. (2003) *Eng Geol*, 68, 319-331. [16] Aydan O. and Ulusay R. (2003) *Eng Geol*, 69, 245-272. [17] Neuffer D. P. et al. (2004) *Eos Trans. AGU*, 85(47), Abstract #V43B-1425. [18] Hoek E. and Brown E. T. (1997) *Int J Rock Mech & Min Sci*, 34, 1165-1186. [19] Okubo C. H. et al. (2004) *Comp & Geosci*, 30, 59-72. [20] Wells D. L. and Coppersmith K. J. (1994) *BSSA*, 84, 974-1002. [21] Joyner W. B. and Boore D. M. (1981) *BSSA*, 71, 2011-2038. [22] Witbeck N. E. et al. (1991) *USGS MI Series*, Map I-2010.

Abstract published in: Lunar and Planetary Science XXXVI, CD-ROM, Lunar and Planetary Institute, Houston (2005).